Numerical Parametric Study on Time-Dependent Response of Geocell-Reinforced Flexible Pavements

Anjana R. Menon and Anjana Bhasi

Abstract Flexible pavements on weak soil are prone to longitudinal cracking and rut formation on the surface. Geocell-reinforced granular layers offer enhanced load distribution and restrict settlement on the pavement under regular vehicular traffic. An intensive parametric study was done to assess the degree of impact of various factors on the time-dependent behavior of flexible pavement with a geocell-reinforced granular base. Parameters analyzed include stiffness and aspect ratio of geocell, frictional characteristics of the granular layer, and subgrade shear strength. The independent effect of each influential parameter on the mechanism of load transfer was analyzed using three-dimensional modeling incorporating the actual honeycomb shape of the geocell. The load transfer mechanism in a geocell is most affected by the tensile stiffness of geosynthetic material and the aspect ratio of the cellular pocket. While the effect of the wide slab mechanism is affected by the strength characteristics of all pavement layers, including fill friction, subgrade cohesion, and geosynthetic stiffness, the membrane effect is dependent purely on the strength and aspect ratio of the geocell. The aspect ratio close to unity is desirable for efficient and uniform stress transfer through Geocell walls.

Keywords Geocell · Honeycomb shape · Repetitive loading · Parametric study · Load transfer mechanism

1 Introduction

Geocells are becoming increasingly popular among civil engineers worldwide due to their versatile applications and ease of installation. Some of the significant fields of application of geocell reinforcement include foundations, embankments, retaining

A. R. Menon (✉) · A. Bhasi
NIT, Calicut, Kerala, India
e-mail: anjana5193@gmail.com

A. Bhasi
e-mail: anjanabhasi@nitc.ac.in

N. Nagabhatla et al. (eds.), *Recent Developments in Water Resources and Transportation Engineering*, Lecture Notes in Civil Engineering 353,
https://doi.org/10.1007/978-981-99-2905-4_21

walls, pavements, and slope stability [1–3]. The load transfer mechanism of geocell involves two principles: membrane action and wide slab mechanism. The membrane action of the geocell is contributed by the vertical component of shear strength mobilized by the geocell walls upon external loading, owing to the resistance of the membrane to bending action [2, 4]. The wide slab mechanism, also called the vertical stress dispersion effect, arises due to the increased rigidity of the geocell-soil composite. The rigid slab-like structure formed by the geocell-infill composite increases the load dispersion angle through the geocell layer, thus increasing the effective stress distribution area on the underlying subgrade [2, 5]. Gedela et al. [6] studied the load dispersion mechanism of geocell-reinforced foundations and analyzed the influence of various factors on the degree of improvement using digital imaging techniques. The significant factors influential in geocell-reinforced systems' behavior include the geocell's strength, geometry, and characteristics of the host soil material in which the geocell is embedded [7–9]. Flexible pavements on soft subgrades demand a reinforcement mechanism to reduce the imbibed stress on the subgrade. Geocell-reinforced granular layer helps in subgrade stress reduction and provides a rigid undulating platform that mitigates settlement-induced cracking on the surface, thus increasing the pavement's service life [10]. The conventional design based on Burmister's layer theory can be modified to incorporate the effect of geocell reinforcement. It is assumed that the geocell reinforcement improves the elastic modulus of the granular layer by a factor that is quantified based on infill strength, subgrade strength, and position of the geocell [11]. In the last few decades, natural geotextiles are gaining popularity in several applications including pavements [12]. But the long-term feasibility can be assured only by using suitable surface treatment to enhance the durability of the fibers [13, 14]. It is to be noted that the initial cost of geosynthetic reinforced pavements is inevitably higher than the unreinforced case due to the additional material cost. However, the reduced maintenance cost owing to increased durability and possible reduction in design layer thickness can compensate for this, in the life cycle assessment. However, there are minimal studies on the time-dependent response of Geocell-reinforced flexible pavements. Since pavements are designed for 5–10 years, and the load is dynamic, the time-dependent response of pavement is significant. Considering various influential factors, the dependence rate on each factor is vital in optimizing the design to suit the field conditions. In the present study, the degree of impact of several influential factors on the Time-dependent behavior of geocell-reinforced flexible pavement is assessed using three-dimensional modeling. The actual curvature of honeycomb-shaped pockets is traced from the scaled-down specimen for accurate simulation of the load transfer mechanism [15]. The effect on wide slab mechanism and membrane effect is analyzed separately about time to provide guidelines for geocell-reinforced flexible pavement design.

2 Materials and Methods

A three-dimensional model of a hypothetical pavement section is developed using the finite element package ABAQUS [16]. The model details and analysis procedure are explained in the subsequent sections.

2.1 Model Geometry and Loading

Basic model geometry: The analysis is performed on a 5 m wide stretch of pavement laid on a soft subgrade overlain by a granular base layer of 0.7 m thickness and surface asphalt course 0.1 m thick. The base is reinforced using Geocell, having a pocket opening size of 0.5 m. To trace the geocell dimensions, a scaled-down specimen was manufactured using a polypropylene-based non-woven geotextile procured from Geodukan [17]. The honeycomb-shaped pockets were developed by stitching the geotextile material in a transverse direction at regular intervals. The coordinates of a single pocket were carefully traced and replicated using ABAQUS to generate the model of the geocell network. Figure 1 shows the laboratory prototype and numerical model of the geocell adopted in the study. The properties of materials used in the basic model are listed in Table 1.

Loading and boundary conditions: Repetitive wheel loads are the most frequent loads on flexible pavement, and pavement response depends on the wheel configuration and traffic intensity. For the present study, cumulative traffic of 100 MSA is considered, and the pavement thickness is based on respective guidelines by IRC [18]. Table 2 shows the wheel configurations and loading characteristics adopted for

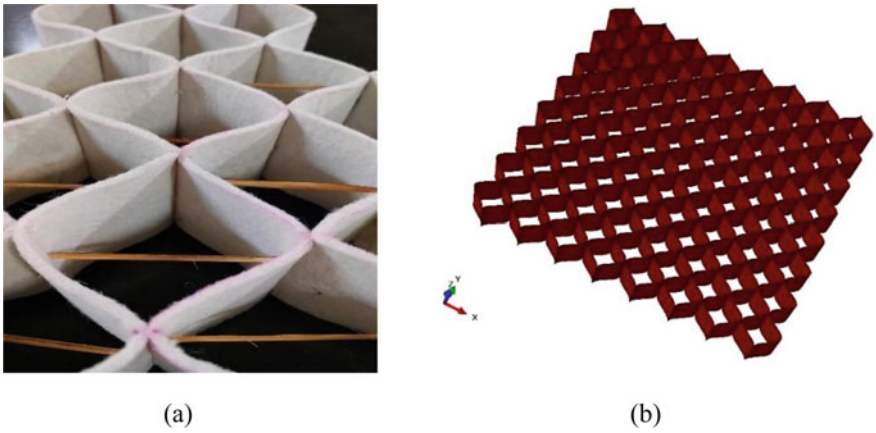

Fig. 1 Geocell used in the study: **a** laboratory prototype and **b** numerical model

Table 1 Material properties used in the basic model

Parameter	Infill material (B)	Subgrade (S)	Geocell (G)
Density (kg/m^3)	1470	1450	200
Friction angle (°)	39	5	–
Elastic modulus (kPa)	57,900	10,600	3.3×10^7
Cohesion (kPa)	–	120	–
Height (m)	0.7	–	0.2

the model analysis. The tire configuration and contact pressure were adopted from Continental Tires [19].

Figure 2 shows the actual elliptical contact area of a wheel and the equivalent rectangular contact area adopted in the model [21]. Each wheel load was applied for a time of 0.01 s and repeated for 1000 continuous cycles. The subgrade bottom was restrained against all movements, whereas the lateral boundaries of the section were assigned roller boundaries to permit vertical deformation alone.

Mesh characteristics: The subgrade and granular base were assumed to behave in a linearly elastic-perfectly plastic manner adopting the Mohr–Coulomb failure criterion. In contrast, the behavior of the asphalt layer and geosynthetic reinforcement

Table 2 Loading characteristics used in the analysis [20]

Characteristic	Value
Traffic (MSA)	100
Wheel load (kN)	40
Contact pressure (kPa)	595
Tire dimensions (length × width) (m)	0.22 × 0.15
Axle distance (m)	1.5

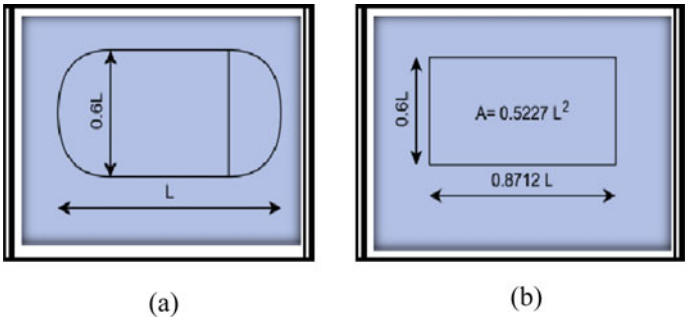

Fig. 2 Wheel contact area: **a** actual elliptical area and **b** equivalent rectangular area [15]

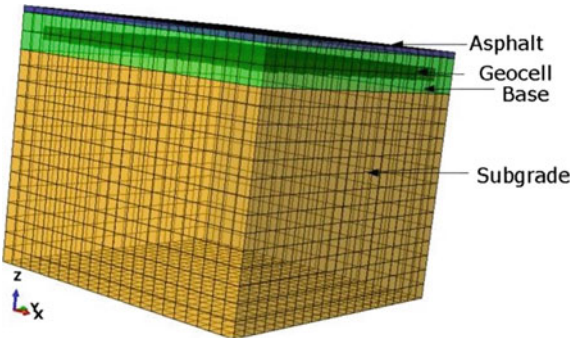

Fig. 3 Numerical model used in the analysis

were assumed to be linear elastic. The pavement layers were modeled as three-dimensional 8-noded linear brick elements with reduced integration (C3D8R). The continuum stress elements are chosen to depict the continuous stress deformation response under loading. The Geocell was modeled using three-dimensional 4-noded membrane elements with reduced integration. (M3D4R). Membrane elements offer zero resistance to bending, thus ideal for simulating the behavior of geosynthetic material. While the geocell, embedded in the granular layer, was assigned hard contact without separation, the different pavement layers were connected using general contact with zero slip and zero separation conditions. Figure 3 shows the profile of the model.

2.2 Parametric Study

Geocell-reinforced soil is a complex system dependent on many factors like subgrade characteristics, base material, and the strength and geometry of geocell. In the present study, the time-dependent response of geocell-reinforced flexible pavement is analyzed by varying the properties of infill material, subgrade, and geocell. The basic model is developed using the material attributes listed in Table 1. For the parametric studies, each parameter was varied at a time to assess the independent effect of individual factors. It is to be mentioned that while varying a fundamental property like the density of fill material, the associated properties like friction angle and elastic modulus vary. Hence, the complete set of properties of the material was varied in each trial for accurate simulation of the modified material characteristics, as summarized in Table 3. It is to be noted that, unlike the conventional studies on reinforced pavements, reduction in thickness is not analyzed in the study because a minimum thickness of 0.7 m is required for embedding the geocell of height 0.5 m. Instead, the study presents the variation in the degree of improvement in stress transfer and deformation under various geocell configurations and material characteristics. The material characteristics are assumed to be constant throughout the analysis. However,

the effect of each parameter on the response of the material is analyzed in terms of the stress deformation response of individual layers.

The height of the geocell varied from 0.5 m to 0.4 m and 0.2 m, mentioned as High (H), Medium (M), and Low (L), respectively. For each height, the influence of each material—Subgrade, Geocell, and Base—was studied by varying one factor at a time, as indicated by the trial name in Table 4.

The material properties of infill material and subgrade are based on laboratory tests. The whole set of analyses was repeated for different geocell heights, 0.2 m, 0.4 m, and 0.5 m (Fig. 4) for a comprehensive assessment of the impact of the aspect ratio of the geocell.

Table 3 Summary of parameters analyzed in the study

Parameter	Infill material			Subgrade			Geocell		
Trial	B_1	B_2	B_3	S_1	S_2	S_3	G_1	G_2	G_3
Density ($kg/m^{3)}$	1470	1296	415	1200	1450	1980	80	200	250
Friction angle (°)	42	39	20	–	–	–	–	–	–
Elastic modulus (MPa)	59	37	83.3	9.6	10.6	14.5	1×10^4	3×10^4	5×10^4
Cohesion (kPa)	–	–	–	80	120	240	–	–	–

Table 4 Summary of model analysis

Geocell height (m)	Low (L) h = 0.2	Medium (M) h = 0.4	High (H) h = 0.5
Trial name	LB_1SG	MB_1SG	HB_1SG
	LB_2SG	MB_2SG	HB_2SG
	LB_3SG	MB_3SG	HB_3SG
	$LBSG_1$	$MBSG_1$	$HBSG_1$
	$LBSG_2$	$MBSG_2$	$HBSG_2$
	$LBSG_3$	$MBSG_3$	$HBSG_3$
	LBS_1G	MBS_1G	HBS_1G
	LBS_2G	MBS_2G	HBS_2G
	LBS_3G	MBS_3G	HBS_3G

L—Low; M—Medium; H—High; B—Base; S—Subgrade; G—Geocell

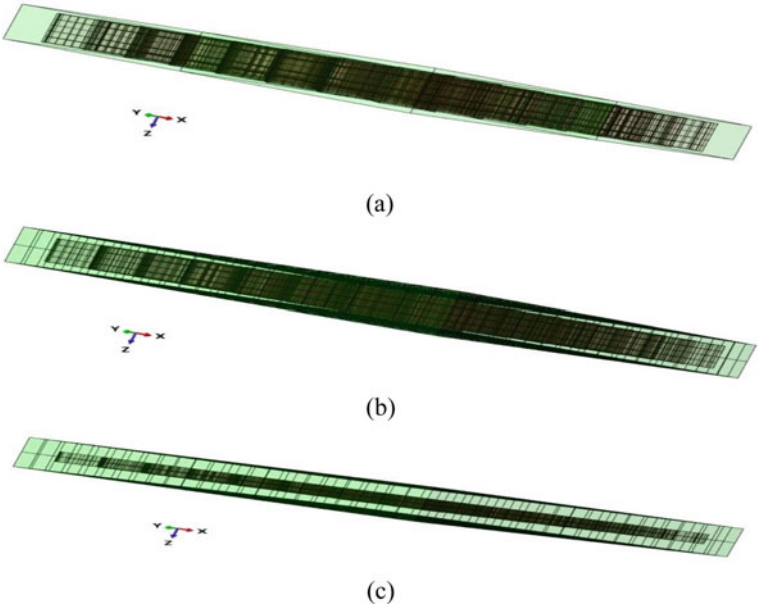

Fig. 4 Geocell of height: **a** 0.5 m-H, **b** 0.4 m-M, and **c** 0.2 m-L

3 Results and Discussion

The time-dependent behavior of flexible pavement is analyzed concerning the two primary mechanisms of load transfer in geocell-wide slab effect and membrane action. The wide slab effect refers to the rigid slab-like action of soil-geocell composite that widens the load dispersion angle, which is reflected in the stress on the underlying subgrade. The membrane action pertains to the tensile stress mobilized on the surface, enabling the membrane to take up a proportion of the imposed load. Each performance aspect is assessed under three different aspect ratios of geocell for the effect of various influential factors like base material properties, stiffness of reinforcement, the strength of subgrade, and height of geocell. In addition, the deformation at the wearing surface and geocell walls after 1000 cycles of loading are also portrayed for geocell reinforcement of various heights.

3.1 Deformation of Subgrade

The deformation characteristics of the subgrade are depicted using maximum vertical strain developed at the surface of the subgrade over time.

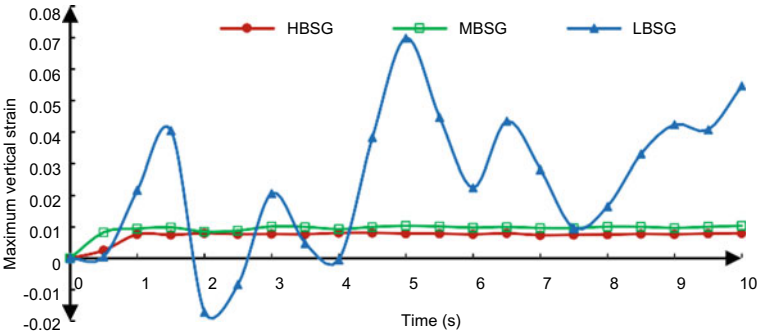

Fig. 5 Effect of the height of geocell on subgrade deformation

Effect of the height of geocell: Fig. 5 presents the effect of the height of the geocell on the time-dependent variation of maximum vertical strain developed at the subgrade. At medium and high wall heights, the maximum vertical strain developed remains nearly constant over time, slightly increasing with a decrease in wall height. However, for a low wall height of 0.2 m, there is a severe fluctuation of vertical strain, and the average strain value is much higher. With an aspect ratio as low as 0.4, the wide slab mechanism is not much efficient since the low walls fail to form a rigid mat. Hence, the efficiency of the geocell is insignificant. The slab action comes into effect at an aspect ratio of 0.8, with the strain almost uniform after the initial loading cycles. The strain further decreases when the aspect ratio becomes unity and remains stable after about 100 cycles of loading. However, considering the meager variation in strain levels, an optimum aspect ratio of 0.8 can be adopted in practice.

Effect of base material characteristics: Fig. 6a–c shows the effect of base material characteristics on maximum vertical strain developed at the subgrade surface over time for the pavement section with High, Medium, and Low-height geocell, respectively. It can be seen that for denser base material with high friction angle, the maximum strain is less. With an increase in friction, the interface friction characteristics also improve, leading to a rigid soil-geocell composite compared to the loose fill with low friction angle. Notably, the deformation profile is undulating in the case of low-height geocell. When the height of the geocell is too low compared to the depth of the embedded layer, the slab action is negligible. As a result, there is less uniformity in the magnitude of stress transferred to the subgrade and the resultant deformation.

Effect of stiffness of geocell: Fig. 7a–c shows the effect of geosynthetic stiffness on maximum vertical strain developed at the subgrade surface over time for the pavement section with High, Medium, and Low-height geocell, respectively. In all cases, the vertical strain on the subgrade is the minimum for the stiffest reinforcement and vice versa. The shear stress mobilized on the reinforcement is proportional to the axial stiffness of the material, thus reflected in the stress transferred to the subgrade and the resultant deformation. The trend aligns with the fact that the immediate settlement

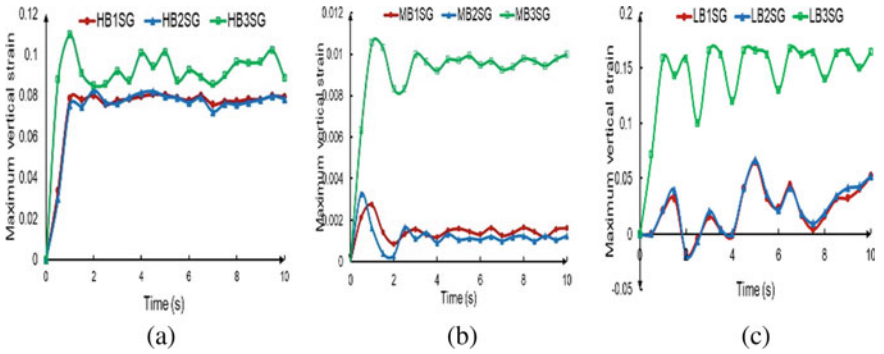

Fig. 6 Effect of granular base properties on subgrade deformation for **a** high, **b** medium, and **c** low geocell heights

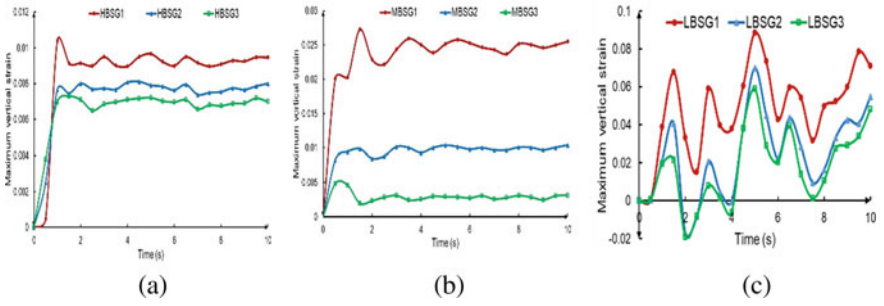

Fig. 7 Effect of stiffness of geocell on subgrade deformation for **a** high, **b** medium, and **c** low geocell heights

of cohesive soil is inversely proportional to the Elastic modulus, an indicator of the material's frictional characteristics. The undulations in the case of Low geocell again reflect the inefficiency of low wall height in the stress transfer.

Effect of subgrade strength: The effect of subgrade strength on maximum vertical strain developed at the subgrade surface over time for the pavement section with High, Medium, and Low-height geocell is shown in Fig. 8a–c, respectively. The magnitude of deformation is inversely proportional to subgrade cohesion, but the pattern is seen to be unaffected. The deformation pattern indicates that the subgrade settles at the first load cycle and remains uniform.

3.2 Surface Deformation

Figure 9 shows the surface deformation after 1000 cycles of loading for various types of geocell reinforcement. Though the pattern is similar, the improved performance

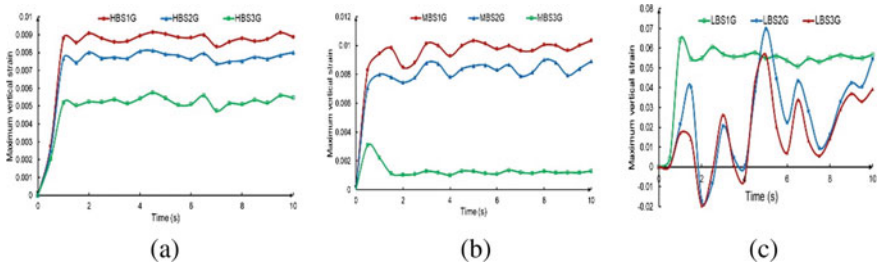

Fig. 8 Effect of subgrade strength on subgrade deformation for **a** high, **b** medium, and **c** low geocell heights

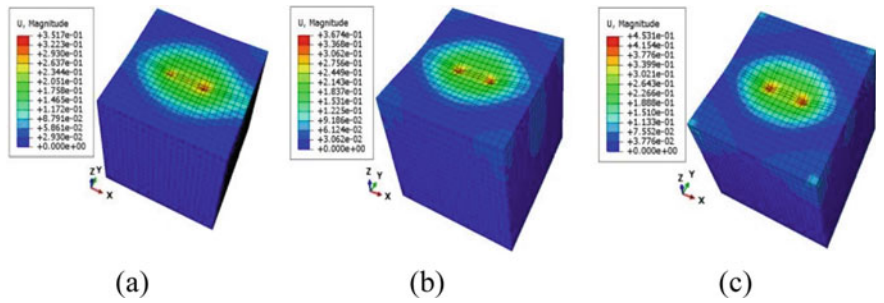

Fig. 9 Surface deformation after 1000 cycles of loading for **a** high, **b** medium, and **c** low geocell heights

of the High wall geocell is reflected in the magnitude of deformation at the wearing surface.

3.3 Membrane Action of Geocell

Membrane action is one of the major load transfer mechanisms in a geosynthetic reinforcement. It refers to the shear strength mobilized on the surface of the geosynthetic upon loading. The membrane develops tensile stress, which helps it to take up the imposed stress. In this study, the influence of various parameters on membrane action is analyzed in terms of the shear stress mobilized on the geocell walls.

Effect of height of geocell: Fig. 10 presents the effect of the wall height of the geocell on the maximum shear stress developed on the geocell.

The membrane action is found to be directly related to the geometry. The increase in the wall height of the geocell elevates the effective area contributing to the tensioned membrane action, which is reflected as higher shear stress on the membrane. However, the pattern of stress remains unaffected.

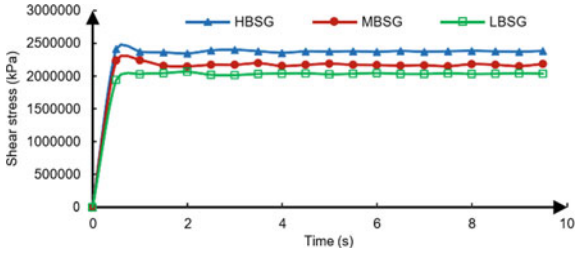

Fig. 10 Effect of the height of geocell on shear strength mobilized on geosynthetic

Effect of the base material characteristics: The influence of granular base material characteristics on the shear stress mobilized in the geocell is shown in Fig. 11a–c for High, Medium, and Low-height geocells, respectively. It is noted that the membrane action is not much affected by the frictional characteristics of base material, albeit with a slight increase in shear stress. Similar observations have been cited by previous studies indicating the insignificant effect of infill material on the behavior of geocell-reinforced soil [5]. The shear strength mobilized is higher when the wall height is 0.5 m, as summarized in Fig. 12.

Effect of stiffness of geocell: The axial stiffness of the material is a factor that directly impacts the membrane action. The higher the stiffness, the higher the shear stress mobilized on the material's surface, as shown in Fig. 12a–c. The increase in stiffness of the material indicates higher resistance to load-induced deformation. In other words, shear stress developed on the material against induced deformation is higher for a stiffer material.

Effect of subgrade strength: Subgrade characteristics significantly impact geocell membrane action, as indicated by Fig. 13a–c. The geosynthetic reinforcement is placed in the overlying granular layer. Hence, the stress developed on the membrane due to external load is unaffected by the underlying soil characteristics.

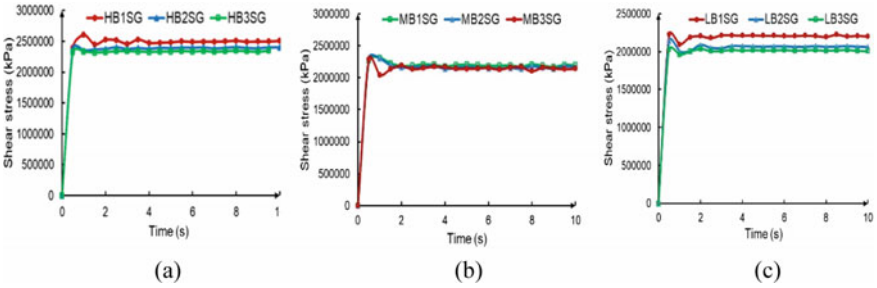

Fig. 11 Effect of properties of the granular base on shear strength mobilized on geosynthetic for **a** high, **b** medium, and **c** low geocell heights

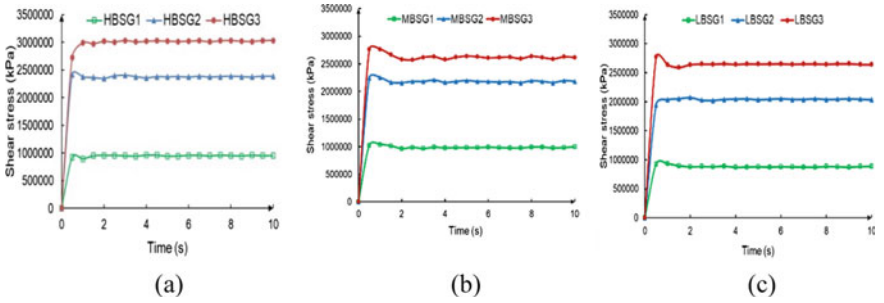

Fig. 12 Effect of stiffness of reinforcement on shear strength mobilized on geosynthetic for **a** high, **b** medium, and **c** low geocell heights

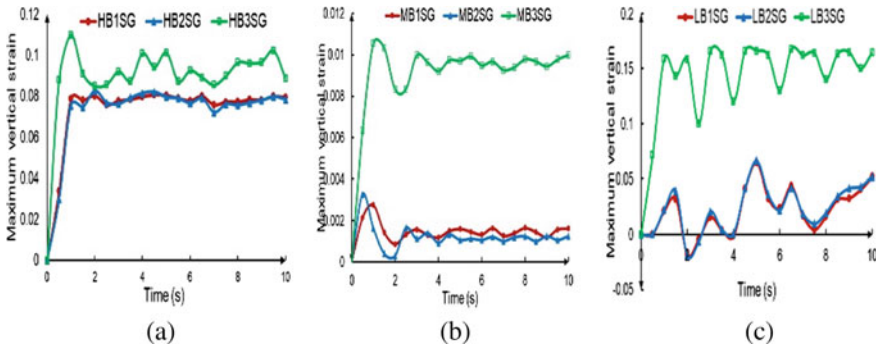

Fig. 13 Effect of subgrade strength on shear strength mobilized on geosynthetic for **a** high, **b** medium, and **c** low geocell heights

3.4 Deformation of Geocell Walls

The deformation pattern of geocell walls indicates the extent of membrane stress developed on the walls. It can be seen that even if the stiffness of the geosynthetic is the same, the deformation magnitude is higher for the low-height geocell, indicating the significance of the aspect ratio of the geocell, which refers to the height-to-diameter ratio of the pockets. For a wall height of 0.2 m, the aspect ratio is as low as 0.4. The overall rigidity of the walls is less in this case, which is reflected as excessive deformation (Fig. 14).

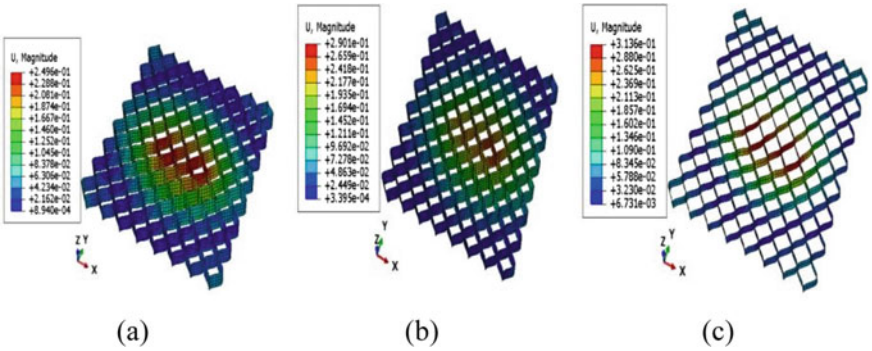

Fig. 14 Deformation of geocell after 1000 cycles of loading for **a** high, **b** medium, and **c** low geocell heights

4 Conclusions

Three-dimensional models of a flexible pavement section with geocell-reinforced granular base were assessed for time-dependent response under a standard repetitive wheel load. The effect of material characteristics and geocell geometry on the geocell-reinforced layer's two primary load transfer mechanisms, namely the wide slab action and the membrane effect, was analyzed over time. The observations lead to the following conclusions:

- The wide slab mechanism of geocell reinforcement helps the uniform load transfer to a broader area toward the subgrade, reflected in the subgrade deformation pattern. The maximum vertical strain in the subgrade varies inversely with friction angle and density of granular base material.
- The strain fluctuation with time is high for geocell with a low aspect ratio. As the aspect ratio approaches unity, the strain variation over time is negligible. Considering economy and efficiency, a minimum aspect ratio of 0.8 can be adopted in practice. Furthermore, the load transfer mechanism is not much affected by the characteristics of the infill material.
- The increase in geosynthetic stiffness and subgrade cohesion improves the stress response of the subgrade, the degree of impact being proportional to the height of the geocell wall. A soft subgrade suffers a higher immediate settlement, with the elastic expansion being lower than that of a stiff subgrade.
- The membrane action is observed to be purely a function of the stiffness and geometry of the geosynthetic material. It is independent of the characteristics of pavement layers, either the subbase or the subgrade. The maximum shear stress developed is low for the low axial stiffness of the geocell and is unaffected by the aspect ratio of the geocell. As the geosynthetic stiffness increases, the slab action is more effective, and the performance is a function of the aspect ratio of the geocell.

- The deformation of geocell walls and the surface deformation are a function of the aspect ratio of the geocell. An optimum height-to-diameter ratio of 0.8 is desirable for uniform deformation and stress transfer.

5 Scope for Future Studies

- The present study is focused on the effect of various internal factors, mainly material characteristics and geometry, on the time-dependent response of geocell-reinforced pavements. Considering the minimum thickness of the granular layer for embedding the geocell, the reduction in design thickness is not included. Thus, a cost analysis is irrelevant in this research and hence excluded. However, the study's findings can be used for a comprehensive analysis of the life cycle assessment of geocell-reinforced pavements in the future.
- The study's findings can be incorporated into the design methodology considering the effect of various parameters analyzed in this article. The modified design extended to field studies is vital in assessing the practical implications of geocell-reinforced pavements.

References

1. Vibhoosha MP, Bhasi A, Nayak S (2021) A review on the design, applications, and numerical modeling of geocell reinforced soil. Geotech Geol Eng 39(6):4035–4057. https://doi.org/10.1007/s10706-021-01774-3
2. Hegde A (2017) Geocell reinforced foundation beds-past findings, present trends, and future prospects: a state-of-the-art review. Constr Build Mater 154:658–674. https://doi.org/10.1016/j.conbuildmat.2017.07.230
3. Mamatha KH, Dinesh SV (2019) Performance evaluation of geocell-reinforced pavements. Int J Geotech 13(3):277–286. https://doi.org/10.1080/19386362.2017.1343988
4. Zhang L, Zhao M, Shi C, Zhao H (2010) Bearing capacity of geocell reinforcement in embankment engineering. Geotext Geomembr 28(5):475–482. https://doi.org/10.1016/j.geotexmem.2009.12.011
5. Menon AR, Konnur S, Bhasi A (2021) Model tests on coir geotextile-encased stone columns with tyre crumb-infilled basal coir geocell. Int J Geosynth Ground Eng 7(2):1–13. https://doi.org/10.1007/s40891-021-00274-x
6. Gedela R, Kalla S, Sudarsanan N, Karpurapu R (2021) Assessment of load distribution mechanism in geocell reinforced foundation beds using digital imaging correlation techniques. Transp Geotech 31:100664. https://doi.org/10.1016/j.trgeo.2021.100664
7. Choudhary AK, Dash SK (2021) Influence of soil density on performance of geocell-reinforced vertical anchor in sand. Geosynth Int 28(4):338–349. https://doi.org/10.1680/jgein.20.00047
8. Kabiri Kouchaksaraei M, Bagherzadeh Khalkhali A (2020) The effect of geocell dimensions and layout on the strength properties of reinforced soil. SN Appl Sci 2(10):1–13. https://doi.org/10.1007/s42452-020-03480-w
9. Jayamohan J, Aparna S, Sasikumar A (2019) Influence of properties of infill material on the behaviour of geocells. In: Ground improvement techniques and geosynthetics. Springer, Singapore, pp 57–66. https://doi.org/10.1007/978-981-13-0559-7_7

10. George AM, Banerjee A, Puppala AJ, Saladhi M (2021) Performance evaluation of geocell-reinforced reclaimed asphalt pavement (RAP) bases in flexible pavements. Int J Pavement Eng 22(2):181–191. https://doi.org/10.1080/10298436.2019.1587437
11. Saride S, Baadiga R, Balunaini U, Madhira MR (2022) Modulus improvement factor-based design coefficients for geogrid-and geocell-reinforced bases. J Transp Eng Part B: Pavements 148(3):04022037. https://doi.org/10.1061/JPEODX.0000380
12. Kumar N, Kandasami RK, Singh S (2022) Effective utilization of natural fibres (coir and jute) for sustainable low-volume rural road construction–a critical review. Constr Build Mater 347:128606. https://doi.org/10.1016/j.conbuildmat.2022.128606
13. Ghosh M, Saha R, Das M (2021) Application of jute-polypropylene blended geotextile in black cotton soil subgrade for low volume road construction. Int J Geosynth Ground Eng 7(3):1–8. https://doi.org/10.1007/s40891-021-00316-4
14. Jiniraj RB, Jayasree PK, Anusha SP (2022) Effect of surface modification on the performance of natural fibres—a review. Ground Improv Reinf Soil Struct 609–615. https://doi.org/10.1007/978-981-16-1831-4_54
15. Hegde AM, Sitharam TG (2015) Three-dimensional numerical analysis of geocell-reinforced soft clay beds by considering the actual geometry of geocell pockets. Can Geotech J 52(9):1396–1407. https://doi.org/10.1139/cgj-2014-0387
16. Simulia (2016) Abaqus/CAE user's manual. Version 6.14
17. http://geodukan.in/
18. IRC:37 (2018) Guidelines for the design of flexible pavements, Indian roads congress, New Delhi pp, pp 19–37
19. https://www.continental-tires.com
20. Arvin MR, Rezaei E, Bahmani Shoorijeh M (2018) Numerical evaluation of geocell-reinforced flexible pavements under traffic loads. Sci Iran 25(2):493–504. https://doi.org/10.24200/sci.2017.4191
21. Huang YH (2004) Pavement analysis and design. Pearson Prentice Hall, Inc. Upper Saddle River, NJ 07458, pp 8–530